Phe393 Mutants of Cytochrome P450 BM3 with Modified Heme Redox Potentials Have Altered Heme Vinyl and Propionate Conformations†

Zhucheng Chen,‡ Tobias W. B. Ost,§ and Johannes P. M. Schelvis*,‡

Department of Chemistry, New York University, 31 Washington Place, Room 1001, New York, New York 10003, and School of Chemistry, Science and Engineering College, University of Edinburgh, West Mains Road, Edinburgh EH9 3JJ, United Kingdom

Received May 29, 2003; Revised Manuscript Received December 16, 2003

ABSTRACT: It has been well established that the heme redox potential is affected by many different factors. Among others, it is sensitive to the proximal heme ligand and the conformation of the propionate and vinyl groups. In the cytochrome P450 BM3 heme domain, substitution of the highly conserved phenylalanine 393 results in a dramatic change in the heme redox potential [Ost, T. W. B., Miles, C. S., Munro, A. W., Murdoch, J., Reid, G. A., and Chapman, S. K. (2001) *Biochemistry 40*, 13421−13429]. We have used resonance Raman spectroscopy to characterize heme structural changes and modification of heme interactions with the protein matrix that are induced by the F393 substitutions and to determine their correlation with the heme redox potential. Our results show that the Fe−S stretching frequency of the 5-coordinated, high-spin ferric heme is not affected by the mutations, suggesting that the electron density in the Fe−S bond in this state is not affected by the F393 mutation and is not a good indicator of the heme redox potential. Substrate binding perturbs the hydrogen bonding between one propionate group and the protein matrix and correlates to both the size of residue 393 and the heme redox potential. However, heme reduction does not affect the conformation of the propionate groups. Although the conformation of the vinyl groups is not affected much by substrate binding, their conformation changes from mainly out-of-plane to predominantly in-plane upon heme reduction. The extent of these conformational changes correlates strongly with the size of the 393 residue and the heme redox potential, suggesting that steric interaction between this residue and the vinyl groups may be of importance in regulating the heme redox potential in the P450 BM3 heme domain. Further implications of our findings for the change in redox potential upon mutation of F393 will be discussed.

Cytochromes P450[1] are a superfamily of heme *b*-containing monooxygenase enzymes, in which a cysteine thiolate acts as the proximal heme ligand (*1*, *2*). They are widespread in all forms of life and notable for their diversity in biosynthetic and degradative pathways in these organisms (*3*, *4*). Cytochrome P450 BM3 (CYP102) is a soluble bacterial enzyme from *Bacillus megaterium*, which catalyzes long-chain fatty acid hydroxylation. It has received much attention recently because of its availability and strong similarity to the physiologically important mammalian P450 enzymes (*3*). Sequence comparison of all P450s reveals that only a few residues are implicitly conserved throughout the superfamily. One is the cysteine that coordinates to the heme iron, Cys400 in P450 BM3 (5). Phe393 in P450 BM3 is almost completely conserved within the "heme binding" motif and locates close to the cysteine ligand and the heme plane (*6*). The high level of conservation underscores the importance of this residue. Previous studies have shown that F393 exerts thermodynamic control over the enzymatic activity in P450 BM3 (*7*). Mutation of this residue results in a lower overall enzyme turnover without obviously altering substrate binding, the product profile, or the extent of uncoupling. Extensive kinetic and thermodynamic characterization has indicated that the change in enzymatic activity can be explained by the difference in heme iron redox potential in the F393 mutants of P450 BM3 with respect to the wild-type enzyme (*7*). On the basis of structural and spectroscopic characterization of the F393H mutant, it was proposed that the increase in heme redox potential is related to weakening of the Fe−S bond, presumably due to either steric or electrostatic interactions between His393 and Cys400 (*8*). The physical origin of the changes in redox properties and the structural basis of thermodynamic control of the redox potential following mutation of F393 remain unclear.

Multiple factors are generally considered to affect the heme redox potential (*9*, *10*), e.g., the microenvironment of the heme cofactor (*11*−*14*), the electrostatic environment (*15*−*17*), heme orientation (*18*, *19*), and nonplanarity of the heme (*20*−*22*). The change in coordination and spin state of the heme iron from water-bound, 6-coordinate, low-spin (6C/LS) to 5-coordinate, high-spin (5C/HS) upon substrate binding is considered to be a switch for physiological heme

† This work was supported by start-up funds from New York University (J.P.M.S.) and by a grant from the BBSRC (T.W.B.O.).

* To whom correspondence should be addressed. Tel.: (212) 998 3597. Fax: (212) 260 7905. E-mail: hans.schelvis@nyu.edu.

‡ New York University.

§ University of Edinburgh.

[1] Abbreviations: 6C/LS, 6-coordinated low-spin; 5C/HS, 5-coordinated high-spin; RR, resonance Raman; Mb, myoglobin; P450, cytochrome P450; CYP102, cytochrome P450 BM3; NOS, nitric oxide synthase; AA, arachidonic acid.

10.1021/bi034920g CCC: $27.50
Published on Web 01/30/2004

reduction and increases the heme redox potential by 100 mV in P450s in general and by 138 mV in P450 BM3 (*7*, *10*). The proximal ligand of the redox center is also believed to play a key role in modifying the redox potential (*23*−*25*), as well as hydrogen bonding to the proximal thiolate ligand (*26*−*29*). The Fe−S bond in P450s has been subject to extensive study (*26*−*34*). Contributions from the heme propionate (*9*, *35*−*40*) and vinyl groups (*18*, *39*, *41*−*43*) have also been considered to play an important role in regulating the heme iron redox potential.

Argos and Matthews originally proposed that the orientation of one propionate group toward the heme iron can stabilize the ferric heme and lower the redox potential (*35*). Extensive work by Mauk and co-workers provided further support for this proposal (*36*−*38*). However, Walker and co-workers showed that no specific propionate contributes to the heme redox potential and that a one carbon change in propionate length had only minimal effect, while removal of one propionate increased the redox potential (*39*). It has been proposed that the total charge near the heme may be important for the heme redox potential (*15*−*17*, *37*−*39*).

Saterlee and Erman observed that rotation of the heme 4-vinyl group and enzyme activity in cytochrome *c* peroxidase have similar pK_a's, presumably by affecting the redox potential (*41*). La Mar et al. concluded that the 2-vinyl group in met-aquo myoglobin is more mobile or has less repulsive interactions with the protein than the 4-vinyl group to keep it in an out-of-plane conformation (*44*). On the basis of model compound studies, it has been proposed that an in-plane vinyl group can withdraw more electron density from pyrrole nitrogens, destabilizing the Fe(III) state in heme proteins and increasing the heme redox potential (*42*). Reid et al. also found that vinyl orientation can influence the heme redox potential by showing that removal of the vinyl groups lowers the heme redox potential by about 49 mV (*43*). A detailed ^{1}H NMR and optical spectroelectrochemical study of modified hemes reconstituted in the soluble fragment of bovine microsomal cytochrome b_5 concluded that the heme redox potential directly correlates to the orientation of the vinyl groups (*39*). These authors noted that vinyl groups can either withdraw or donate electron density and convincingly argued that they withdraw electron density from the heme, the in-plane conformation being the most electron withdrawing. Resonance Raman experiments on P450 BM3 have indicated that the vinyl groups are more mobile compared to those in other P450 isoforms (*45*−*48*), and it was proposed that this could affect enzyme reactivity (*47*, *48*). However, a correlation between heme redox potential and vinyl group orientation has not been established.

In this paper, we want to determine whether changes in the conformation of the heme substituent groups and their interaction with the protein correlate to the modification of the heme redox potential upon mutation of F393. The set of F393 mutants is well suited for such an investigation because only a single residue has been substituted, and the structural changes are expected to be localized. We will use resonance Raman (RR) spectroscopy because it is a powerful tool to detect subtle changes in the interactions between the heme cofactor and its protein environment (*49*). Since the vibrational modes associated with the vinyl and propionate groups and the Fe−S stretching frequency are well-known from the literature (*30*, *32*, *50*−*53*), these important heme−protein interactions can be investigated. Our studies indicate that the Fe−S bond is insensitive to the F393 mutations and that conformational changes of the propionate and vinyl groups correlate to the size of residue 393 and to the heme redox potential in the P450 BM3 F393 mutants. The implication of our observations for regulation of the heme redox potential will be discussed.

MATERIALS AND METHODS

Arachidonic acid and sodium dithionite were purchased from Sigma Chemical Company and used without further purification.

Enzyme Preparation. P450 BM3 enzymes were obtained from a bacterial expression system (*7*) (manuscript describing preparation of the F393W mutant is in preparation). All mutant and wild-type P450 BM3 heme domain proteins were overexpressed in *Escherichia coli* strain TG1. Transformant cultures (2−5 Ls Luria-Bertani medium at 37 °C with shaking at 200 r.p.m) were grown to $A_{600} = 1$ and induced with IPTG (250 μM). Growth was continued for 24 h prior to harvesting cells. Cells were resuspended in 50 mM Tris/1 mM EDTA pH 7.4 (Buffer A) and lysed by sonication. Enzymes were purified by an established protocol employing ion-exchange chromatography (*54*). A final step using a HiLoad 26/10 Q-Sepharose high performance column attached to a Pharmacia FPLC system (elution gradient 0−500 mM KCl in Buffer A) was employed to maximize the final purity of all the proteins. PMSF (1 mM) was added to all buffers to minimize proteolysis. Purified proteins were eluted through a G25 column preequilibrated with Buffer A prior to concentration (>500 μM) by ultrafiltration. Samples were flash frozen in liquid nitrogen and shipped in dry ice. Upon arrival, samples were diluted to 40 μM in Buffer A and stored at −80 °C in smaller volumes for use in the resonance Raman experiments.

Electronic Absorption Spectroscopy. Electronic absorption spectra were obtained at room temperature with a UV−vis spectrophotometer (Lambda P40, Perkin-Elmer) with the sample sealed in a Raman spinning cell. Absorption spectra of all samples were taken to ensure integrity before and after the resonance Raman experiments, and no sample degradation was observed. Absorption spectra of all the samples in both redox states in the presence and absence of substrate are provided in the Supporting Information.

Resonance Raman Spectroscopy. The resonance Raman spectrometer has been described in detail elsewhere (*26*). Holographic notch filters (Kaiser Optical) were used to remove Rayleigh scattering from the Raman signal. The samples were placed in a spinning cell under a N_2 atmosphere and kept at 8±2 °C during the experiments. Laser lines from a Kr^+ (Coherent, I-302) and an Ar^+ laser (Coherent, I-307) were used for excitation of the samples with 10 mW incident laser power unless stated otherwise. The sloping background of the spectra, presumably due to fluorescence of unknown origin and/or the small wavelength dependence of our detector, was flattened, if necessary, by subtraction of a smooth polynomial (3rd to 6th order) that had been fitted to the baseline of the spectrum. Corrected spectra were compared to the raw data to ensure that no artifacts had been generated. Toluene was used to calibrate the spectra, and

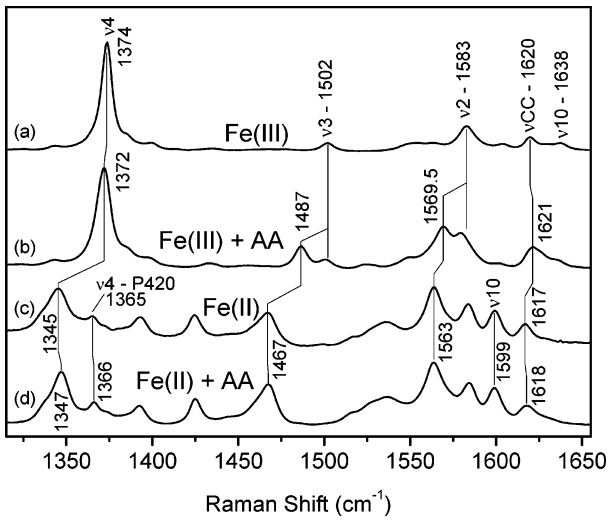

FIGURE 1: High-frequency resonance Raman spectra of the heme domain of wild-type P450 BM3 (40 μM): ferric (a), ferric plus 400 μM arachidonic acid (b), ferrous, reduced with excess dithionite (c), ferrous plus 400 μM arachidonic acid, reduced with excess dithionite (d). Excitation wavelengths: 413.1 (a) and 406.7 nm (b−d).

Table 1: Frequency of the Heme Skeletal Vibrations (cm^{-1}) in the Oxidized and Reduced (r) WT P450 BM3 Heme Domain and Its F393 Mutants with and without Arachidonic Acid (AA)[a]

protein	ν_4 (±0.3)	ν_3 (±0.2)	ν_2 (±0.2)	ν_{10} (±0.3)	ν_{CC} (±0.2)	assignment[b]
F393W	1373.8	1502.3	1583.0	1637.5	1619.2	6C/LS
WT	1373.8	1502.1	1582.8	1637.7	1619.8	6C/LS
F393Y	1373.4	1501.6	1582.7	1636.8	1619.6	6C/LS
F393H	1373.6	1501.7	1582.7	1636.0	1619.4	6C/LS
F393A	1373.2	1501.6	1583.0	1637.1	1621.5	6C/LS
F393W+AA	1371.6	1486.9	1570.2	n.d.[c]	1622.2	5C/HS
WT+AA	1371.9	1486.6	1569.5	n.d.	1621.1	5C/HS
F393Y+AA	1371.5	1486.2	1569.1	n.d.	1621.1	5C/HS
F393H+AA	1371.7	1486.1	1568.1	n.d.	1620.3	5C/HS
F393A+AA	1371.4	1486.6	1569.2	n.d.	1621.9	5C/HS
F393W[r]	1344.8[d]	1467.6[e]	1563.9	1599.7	1616.5	5C/HS
WT[r]	1345.1	1466.8	1563.8	1599.1	1616.9	5C/HS
F393Y[r]	1344.5[f]	1466.8	1562.9	1599.0	1614.8	5C/HS
F393H[r]	1345.4	1466.8[e]	1562.6	1599.7[e]	1616.8	5C/HS
F393A[r]	1347.7	1466.8	1562.8	1598.6	1617.3	5C/HS
F393W[r]+AA	1347.2	1467.6	1563.8	1599.8	1618.3	5C/HS
WT[r]+AA	1347.1	1467.3	1564.2[e]	1599.2	1617.7	5C/HS
F393Y[r]+AA	1346.3	1467.3	1562.4	1598.6	1615.6	5C/HS
F393H[r]+AA	1347.6	1466.9	1562.3	1598.6	1616.5	5C/HS
F393A[r]+AA	1347.9	1466.5	1562.5	1598.4	1616.9	5C/HS

[a] Standard deviation is given between parentheses (cm^{-1}). [b] Assignments following refs *47* and *48*. [c] Not determined (n.d.) because ν_{10} is convoluted with the stretching modes of the vinyl groups. [d] ±1.5 cm^{-1}. [e] ±0.6 cm^{-1}. [f] ±1.7 cm^{-1}.

the vibrations were labeled and assigned according to the literature (*50*−*53*).

RESULTS

High-Frequency RR Spectra of the P450 BM3 *Heme Domain.* High-frequency RR spectra of the WT P450 BM3 heme domain in its oxidized and reduced form in the presence and absence of arachidonic acid are shown in Figure 1. The results for the F393 mutants are similar to those of the WT (Supporting Information) and are listed in Table 1. The ferric heme domains are 6C/LS, as indicated by the frequencies of their ν_4, ν_3, ν_2, and ν_{10} modes (*50*−*53*), and compare well to those reported previously for P450 BM3 (*47*, *55*, *56*). The differences between WT and the F393 mutants are small and cannot be given any significance at this point; e.g., the frequency of the ν_4 vibration varies by only 0.6 cm^{-1}. The vinyl stretching vibration, ν_{CC}, occurs at 1620 cm^{-1}, and its frequency varies slightly among the F393 mutants, being the highest in F393A. A second ν_{CC} mode can be observed at 1632 cm^{-1}, though its intensity is much weaker, especially in F393Y and WT heme domain (Supporting Information). The ν_{CC} vibrations at 1620 and 1632 cm^{-1} can be assigned to in-plane and out-of-plane vinyl conformers, respectively (*57*). The presence of two vinyl conformers in the heme domain of P450 BM3 has been reported before (*47*).

Addition of arachidonic acid in more than 10-fold excess (*7*) converts the WT heme domain to 5C/HS (ν_3 = 1487 cm^{-1}, ν_2 = 1570 cm^{-1}), but some 6C/LS heme (ν_3 = 1502 cm^{-1}, ν_2 = 1583 cm^{-1}) is still observed (Figure 1b). Addition of more substrate did not result in any further spin conversion. Very similar vibrations and mixed heme states have been reported before for the P450 BM3 heme domain in the presence of palmitate and tridecanoate (*47*, *55*) and have also been documented for P450cam and microsomal cytochrome P450 isozymes LM2 and LM4 (*58*−*60*). Complete spin conversion was reported in a surface-enhanced resonance Raman scattering (SERRS) study of P450 BM3 (*46*). This may be due to perturbation of the heme pocket due to protein-metal interactions, because the resting enzyme had already an unusual amount of 5C/HS heme (*46*). The degree of spin-state conversion is different for the mutants as was previously reported (*7*) and can be observed in their absorption spectra (Supporting Information). The WT enzyme has the highest spin conversion, followed by F393W and F393A and by F393Y and F393H (*7*). The ν_{CC} vibration is at 1622 cm^{-1}, and the shoulder at 1635 cm^{-1} is due to the ν_{10} vibration of 6C/LS heme (*50*, *51*). Mutation of F393 causes no significant change in the heme skeletal vibrational frequencies, but their relative intensities in F393W are surprising. Although the UV−vis spectra indicate that it has as much 5C/ HS heme as F393A but less than WT, its intensities of the 5C/HS heme vibrations are much more intense after normalization of the spectra on the ν_4 vibration. The origin of this enhancement is not clear. It was previously shown that the Soret absorption maximum is the same for the substrate-bound heme domains (*7*), but the ligand-to-metal charge transfer (LMCT) band varies from 644 nm in WT to 647 nm in F393W and F393Y, 648 nm in F393A, and 649 nm in F393H (Supporting Information). However, its exact position is difficult to determine, especially in the WT heme domain, because of a sloping baseline.

Although complete reduction of all the samples could be obtained for the UV−vis experiments (*7*, Supporting Information), this could not be fully accomplished in our laboratory for the WT heme domain and the F393W and F393Y mutants in our Raman cells. Autoxidation and photooxidation in laser experiments have been cited as complicating factors (*56*, *59*). The spectra of reduced WT, F393W, and F393Y have been corrected by subtracting the contributions of the oxidized heme. Since the ν_4 vibration is by far the strongest vibration of the oxidized heme domain upon excitation at 406.7 nm, this correction mainly affects the ν_4 vibrational region (1340−1380 cm^{-1}). The high-frequency RR spectrum of the WT heme domain (Figure 1c) is very similar to that previously reported for the P450

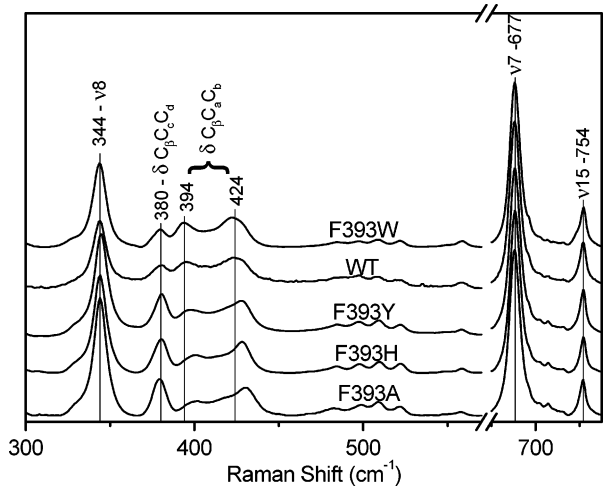

FIGURE 2: Low-frequency resonance Raman spectra of P450 BM3 resting enzyme (40 μM): F393W, wild type (WT), F393Y, F393H, and F393A excited at 413.1 nm.

BM3 holoenzyme and heme domain and to that of other P450s (*47*, *56*, *59*). Upon reduction, the ν_4 vibration is downshifted to 1345 cm^{-1} due to strong $Fe^{II}d_\pi$ back bonding to the porphyrin ring because of strong electron donation of the proximal thiolate to the heme iron (*61*). The ν_3 and ν_2 vibrations are observed at 1467 and 1564 cm^{-1}, respectively (*59*, *61*). Following polarization studies by Wells et al. (*59*), we assign the 1599 and 1584 cm^{-1} vibrations to ν_{10} and ν_{38}, respectively, though the reverse assignment has been proposed (*47*, *61*). Only one ν_{CC} vibration seems present at 1617 cm^{-1}, which suggests that both vinyl groups are more or less coplanar with the porphyrin ring upon heme reduction, as has been proposed before (*47*, *56*). Finally, a small band at 1365 cm^{-1} is due to the inactive, P420 form of the enzyme and is present in all previously reported RR spectra of reduced P450 BM3 (*47*, *56*). Mutation of F393 mainly affects the oxidation state marker, ν_4, which suggests changes in the electron density of the heme iron, it being the highest in F393Y (lower ν_4) and the lowest in F393A (higher ν_4) (*61*). F393Y and F393A have also the lowest and highest ν_{CC} frequency. The other heme skeletal vibrations are not affected significantly by the F393 mutations.

Addition of arachidonic acid does not affect the RR spectrum of the ferrous WT heme domain much (Figure 1d). The ν_4 frequency increases by 2 cm^{-1}, also seen in the F393 mutants (Table 1), and is more similar for the various F393 mutants, though it is still a little lower in F393Y. This frequency increase suggests a decrease in the σ-electron donation from the thiolate ligand to the heme iron following substrate binding (*61*). The ν_{CC} mode also shifts to a higher frequency after addition of substrate and is still the lowest in F393Y. In the substrate-bound form, a ν_4 vibration at 1365 cm^{-1} indicates a small amount of the P420 form is present.

Low-Frequency RR Spectra of Ferric WT and F393 Mutants. In the low-frequency region, Figure 2, the ν_{15}, ν_7, and ν_8 modes of the WT heme domain occur at 754, 677, and 344 cm^{-1}, respectively. The spectral features are very similar to those reported before (*47*, *55*, *62*). The propionate bending mode, $\delta(C_\beta C_c C_d)_{6,7}$, occurs at 380 cm^{-1}, and its frequency is indicative of hydrogen bonding of the propionate groups to well-ordered amino acid residues rather than to more disordered, bulk solvent molecules (*63*−*66*). Two vinyl bending modes, $\delta(C_\beta C_a C_b)_{2,4}$, are observed at 394 and 424 cm^{-1} (*52*, *53*), indicating two distinct vinyl conformations. In myoglobin (Mb), the vinyl bending mode at 440 cm^{-1} was assigned to its 2-vinyl group (*52*), which is rotated more out of the heme plane than the 4-vinyl group (67,68, PDB entries 1YMB and 1WLA), though the X-ray data do not necessarily reflect the conformations populated in solution. In cytochrome *c* peroxidase, a vinyl bending mode at 406 cm^{-1} is associated with a stretching mode at 1618 cm^{-1}, while the one at 418 cm^{-1} corresponds to a stretching mode at 1628 cm^{-1} (*69*). On the basis of these observations and the assignments of the vinyl stretching modes (*57*), we attribute the ~400 cm^{-1} vinyl bending mode to an in-plane vinyl conformer with $\nu_{CC} = 1620$ cm^{-1} and the vinyl bending modes with higher frequencies to out-of-plane vinyl conformers with $\nu_{CC} = 1632$ cm^{-1}.

Mutation of F393 has a negligible effect on ν_8 (less than 1 cm^{-1}) but changes the intensity of the propionate bending mode and the frequencies of the vinyl bending modes significantly. The mechanism that determines the resonance Raman intensity of the propionate bending mode is not known, but we hypothesize that it may be related to the orientation of the propionate groups with respect to the heme plane. The frequencies of the vinyl bending modes increase as follows: F393W < WT < F393Y < F393H < F393A. These frequencies suggest modification of the vinyl conformations and seem to correlate to the heme redox potential and the size of the residue at position 393. The results are summarized in Table 2.

Several weak vibrations are detected around 500 cm^{-1}, which have been assigned to out-of-plane vibrations that are enhanced upon ruffling of the porphyrin ring (*70*). Normalization on the ν_7 vibration shows that the intensities of these modes are somewhat larger for F393Y, F393H, and F393A compared to those for F393W and WT enzyme, which may indicate small differences in heme planarity. However, the absence of significant changes in the high-frequency vibrations of WT and mutant enzymes suggests that the heme plane geometry remains unchanged. Therefore, the F393 mutation induces the most notable changes in the vinyl bending frequencies, suggesting subtle variations in the conformations of the vinyl groups and/or their protein environment.

Addition of arachidonic acid (AA) induces a vibration at 366 cm^{-1} (Figure 3), and we assign it to a new propionate bending mode (*52*, *53*). A lower propionate bending frequency has been associated with perturbation of propionate hydrogen bonding to the protein matrix due to substrate binding (*34*, *63*−*66*, *71*, *72*). Deng et al. have assigned the 366 cm-^{1} mode to γ_6 (*55*). Three observations argue against this assignment. First, the γ_6 vibration in Mb occurs at 337 cm^{-1} (*52*). Second, it is unexpected to observe only a strong γ_6 vibration while other porphyrin out-of-plane modes, such as γ_7 and the modes between 500 and 600 cm^{-1} are weak. Third, we detect the γ_6 vibration at 333 cm^{-1} in the reduced heme domains (vide infra). The relative intensity of the propionate bending mode at 366 cm^{-1} compared to the one at 380 cm^{-1} increases, and therefore, perturbation of the hydrogen-bonding network increases as follows: F393A ~ F393H < F393Y ≤ WT < F393W. This order is not affected by the heme spin-state equilibrium because UV−vis spectra of the samples in the Raman cells (Supporting Information)

Table 2: Low-Frequency Vibrations (cm-[1]) and Heme Iron Redox Potentials of the WT P450 BM3 Heme Domain and Its F393 Mutants with and without Arachidonic Acid (AA)[a]

protein	ν_8 (± 0.3)	$\delta C_\beta C_c C_d$	$\delta C_\beta C_a C_b$	ν(Fe-S)	E_m (mV)[b]
F393W	343.6	380	393,422		−480
WT	344.0	380	394,424		−427
F393Y	344.4	380	395,428		−418
F393H	344.1	380	400,428		−332
F393A	344.3	380	401,430		−312
F393W[r]	363.8[c]	377[sh]	411		
WT[r]	363.4	379[sh]	416		
F393Y[r]	362.8	379	409,424[sh]		
F393H[r]	362.6	379	409,426		
F393A[r]	362.9	380	408,426		
F393W+AA	343.1[d]	366 (0.63),[e] 380 (0.37)	405 (0.09), 415 (0.39), 428 (0.52)	355	−330
WT+AA	343.9	366 (0.53), 380 (0.47)	405 (0.08), 416 (0.33), 428 (0.59)	356	−289
F393Y+AA	344.1	365 (0.46), 380 (0.54)	406 (0.13), 416 (0.24), 429 (0.63)	356	−295
F393H+AA	344.7	364 (0.35), 380 (0.65)	405 (0.11), 416 (0.20), 429 (0.69)	356	−176
F393A+AA	344.4	364 (0.40), 380 (0.60)	406 (0.11), 416 (0.20), 429 (0.69)	355	−151
F393W[r]+AA	364.2	373, 380	408(0.46), 417(0.29), 426(0.25)		
WT[r]+AA	363.8	373, 380	408(0.45), 418(0.28), 426(0.26)		
F393Y[r]+AA	362.9	380	407(0.54), 416(0.14), 426(0.32)		
F393H[r]+AA	362.9	380	407(0.59), 416(0.10), 427(0.31)		
F393A[r]+AA	362.5	380	408 (0.66), 418 (0.03), 426 (0.31)		

[a] Standard deviation is given between parentheses (cm^{-1}). r, sodium dithionite reduced; sh, shoulder. [b] Reference *5*. [c] ±1.2 cm^{-1}. [d] ±0.8 cm^{-1}. [e] Relative integrated intensity between parentheses.

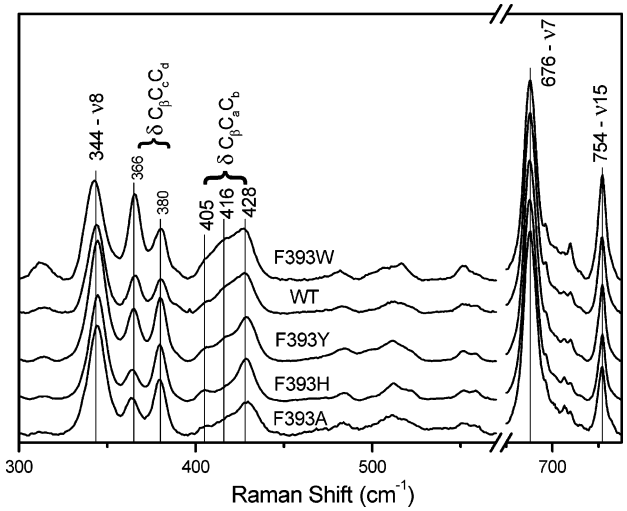

FIGURE 3: Low-frequency resonance Raman spectra of arachidonic acid bound P450 BM3 F393W, wild type (WT), F393Y, F393H, and F393A excited at 406.7 nm. The enzyme concentration was 40 μM with a substrate concentration of 400 μM.

suggest that the relative intensity of the 366 cm^{-1} mode in F393Y and F393H may be underestimated. Therefore, the latter's relative intensity may be higher than in F393A, and the former's may be more similar to that of the WT heme domain. F393W binds slightly less substrate than WT, and the relative intensity of its 366 cm^{-1} mode may be underestimated. Our data suggest a correlation between the size of the 393 residue and the extent of perturbation of the propionate hydrogen-bonding network on addition of substrate. This perturbation is stronger in heme domains with bulkier residues at the 393 position and lower heme redox potentials.

Substrate binding also changes the relative intensities of the vinyl bending modes, and multiple vinyl bending modes persist in substrate-bound P450 BM3, as was previously observed (*47*, *55*). Deconvolution of the vinyl bending mode region in WT heme domain (Supporting Information) reveals the presence of three vibrations at 405, 416, and 428 cm^{-1}, with relative integrated intensities of 8%, 33%, and 59%, respectively. Mutation of F393 affects the relative intensities of these vibrations (Table 2). The 405 cm^{-1} vibration has about 10% of the integrated intensity in all heme domains. An intensity increase of the 428 cm^{-1} mode concomitant with an intensity decrease of the 416 cm^{-1} mode occurs as follows: F393W < WT ~ F393Y < F393H ~ F393A. The intensity increase of the 428 cm-[1] vinyl bending mode indicates an increase in out-of-plane vinyl conformer population with decreasing size of residue 393 and increasing heme redox potential in the substrate-bound heme domain. The ν_8 mode shifts to a slightly higher frequency following the same 393 substitution order, which may be due to its sensitivity to pyrrole-substituent bending coordinates besides to ν(Fe−N) (*52*, *53*).

Detection of Fe−S Vibration. The Fe−S vibration, ν(Fe−S), of hemethiolate enzymes can be detected in the 5C/HS ferric state upon excitation in the Fe−S charge-transfer band (*30*−*32*). Figure 4a shows the low-frequency RR spectra of AA bound WT heme domain excited at 406.7, 356.4, and 363.8 nm. Excitation with 356.4 and 363.8 nm shows a strong, new vibration at 356 cm^{-1}. The excitation profile of this vibration resembles that of ν(Fe−S) in P450cam, which occurs at 351 cm^{-1} (*30*, *32*, *59*). Furthermore, ν(Fe−S) has been detected in other hemethiolate enzymes at 338, 347 and 350 cm^{-1} (*26*, *31*, *34*). Therefore, we attribute the 356 cm^{-1} vibration in AA-bound P450 BM3 heme domain to ν(Fe−S) in the 5C/HS ferric form. In P450 BM3 holoenzyme, it was reported at 346 cm^{-1} (*73*). However, this was probably the ν_8 vibration because 431 nm does not enhance ν(Fe−S) (*32*), and the enzyme was low-spin, in which spin state ν(Fe−S) has only been observed for Cys−His axial ligation (*74*). With SERRS, ν(Fe−S) was reported at 349 cm^{-1}, but protein−metal interactions may have deformed the heme pocket (*46*), resulting in a shift in ν(Fe−S), similar to P450cam when it interacts with putidaredoxin (*33*). Our Fe−S frequency is also higher than that reported by Deng

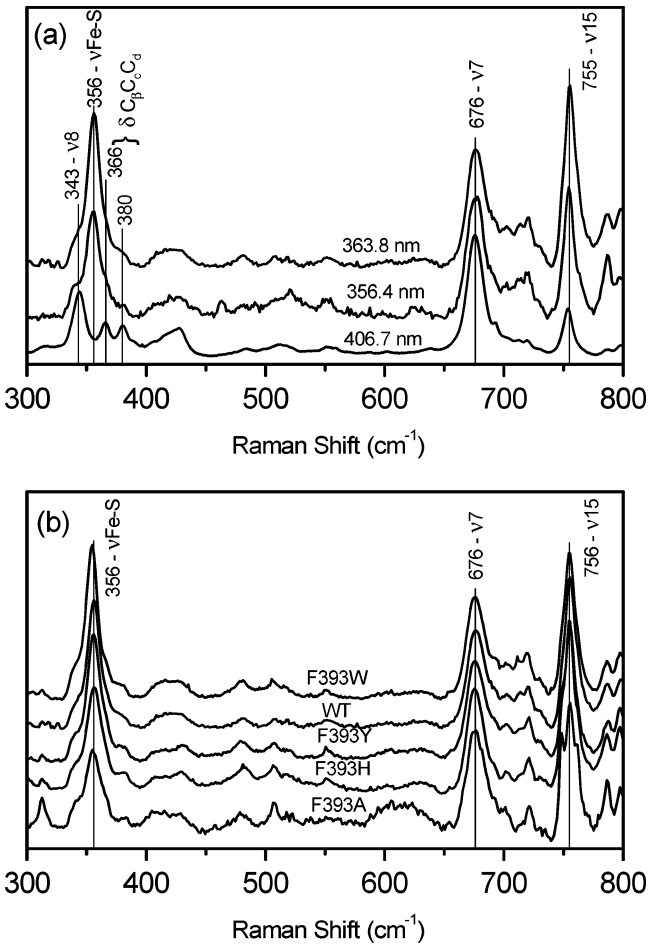

FIGURE 4: Low-frequency resonance Raman spectra of arachidonic acid (400 μM) bound P450 BM3 (40 μM). (a) WT enzyme excited with multiple wavelengths: 406.7, 356.4, and 363.8 nm. (b) F393W, wild type (WT), F393Y, F393H, and F393A excited at 363.8 nm. The spectra excited with 356.4 and 363.8 nm were collected with a laser power of 13 mW.

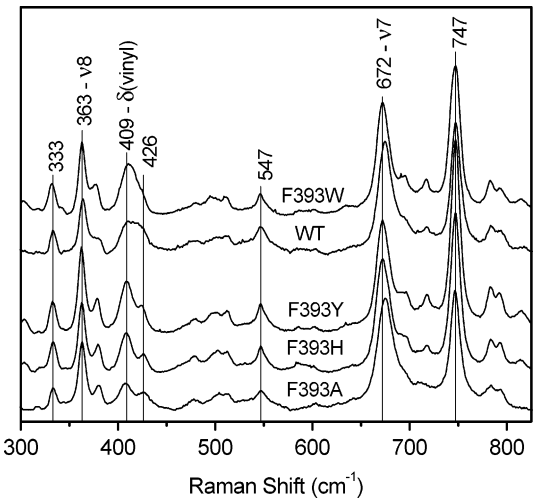

FIGURE 5: Low-frequency resonance Raman spectra of dithionite-reduced P450 BM3 (40 μM) F393W, wild type (WT), F393Y, F393H, and F393A excited at 406.7 nm. The samples were sealed in a Raman spinning cell. After repeating cycles of degassing and filling with N_2 gas for several times, 20 mM sodium dithionite solution was added to reduce the enzymes.

et al. (351 cm^{-1}). The reason for this difference is unclear, though it may be related to the different substrates used (*55*). Mutation of F393 has little effect on the ν(Fe−S) frequency (Figure 4b). It is detected at 356 cm^{-1} in F393Y and F393H, while it is observed at 355 cm^{-1} in F393W and F393A. The fact that the F393 mutations do not significantly affect ν-(Fe−S) indicates that these mutations do not alter the Fe−S bond strength or electron density on the ferric heme iron in the 5C/HS ferric state much. This result is surprising because the mutations do significantly modify the heme redox potential.

Low-Frequency RR Spectra of Ferrous WT and F393 Mutants. The low-frequency spectra of WT, F393W, and F393Y have also been corrected by subtraction of the contributions of oxidized heme after normalization on its ν_8 vibration. This vibration is by far the strongest in the 300 to 600 cm^{-1} region, and the subtraction is not expected to produce artifacts. The ν_8, ν_7, and ν_{15} vibrations are observed at 363, 674, and 747 cm^{-1}, see Figure 5 (*50*, *51*, *59*). The propionate bending mode is observed at 379 cm^{-1}, and the vinyl bending region shows a broad band at 416 cm^{-1}, suggesting an equal population of in-plane and out-of-plane vinyl conformers, which is a change from the oxidized WT heme domain with a predominant out-of-plane vinyl conformation. The vibration at 333 cm^{-1} is assigned to γ_6, an out-of-plane mode and suggests deformation, probably, ruffling of the heme plane (*52*), which is supported by an intensity increase of the out-of-plane modes between 500 and 600 cm^{-1} (*70*). Mutation of F393 induces a small frequency downshift in ν_8 due to its sensitivity to ν(Fe−N) and pyrrole-substituent bending coordinates (*52*, *53*), in agreement with the upshift in the ν_4 frequency due to changes in thiolate σ-electron donation to the heme iron. The major change occurs in the relative intensities of the vinyl bending modes. F393W shows a broad band at 411 cm-[1], while F393Y, F393H, and F393A have two distinct peaks at 409 and 426 cm^{-1}. This is a clear reversal of the peak intensities compared to the oxidized heme domains and indicates that the vinyl groups now favor a more in-plane conformation in agreement with the single ν_{CC} mode at 1622 cm^{-1} (Figure 1c, *47*, *56*). One-electron reduction of the heme iron seems to result in a change in vinyl conformation from out-of-plane to in-plane, and the extent of this change depends on residue 393.

Addition of arachidonic acid induces a new propionate binding mode at 373 cm^{-1} similar to the oxidized heme domains (Figure 6), indicating perturbation of propionate hydrogen bonding (*63*−*66*). The relative mode intensity with respect to the one at 380 cm^{-1} decreases as follows: F393W > WT > F393Y > F393H ∼ F393A, the same as in the substrate bound ferric heme domains, underscoring the correlation between loss of hydrogen bonding and residue size. Mutation of F393 results in large changes in the vinyl bending modes. Gaussian deconvolution (Supporting Information) shows three vibrations at 408, 418, and 426 cm^{-1} with varying relative integrated intensities (Table 2). Although a small amount of ferric heme may contribute to the spectra as indicated by its ν_8 vibration at 344 cm^{-1}, its intensity, and especially that of its vinyl modes (Figure 3), is small and does not affect our analysis. Similar to the substrate-free heme domains, the ν_8 vibration shifts to a slightly lower frequency due to the F393 mutations.

Comparison of the substrate-bound ferrous and ferric heme domains shows a dramatic change in vinyl conformations.

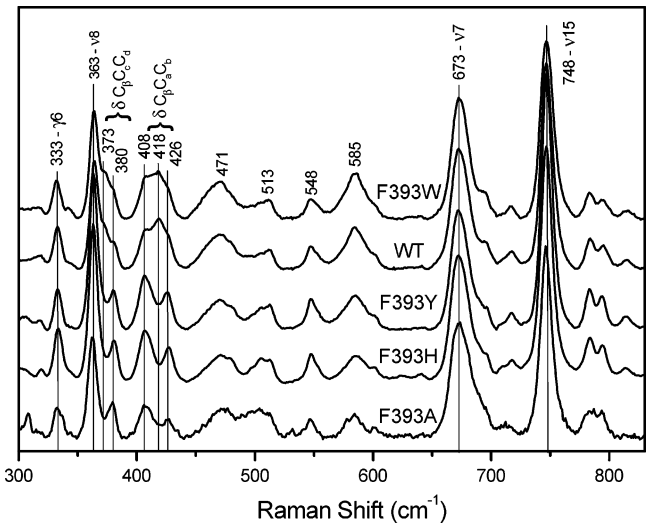

FIGURE 6: Low-frequency RR spectra of arachidonic acid (400 μM) bound, dithionite-reduced P450 BM3 (40 μM) F393W, wild type (WT), F393Y, F393H, and F393A excited at 406.7 nm. The samples were degassed and reduced as described in Figure 5.

Upon heme iron reduction, the vinyl conformation changes from mainly out-of-plane to predominantly in-plane, as was observed before (*52*, *57*, *69*). In the F393H and F393A mutants, the relative integrated intensity of the 408 cm^{-1} mode increases from 10% to 59% and to 66%, respectively, with a concomitant intensity decrease of the 428 cm^{-1} mode from 70% to 30%. The change in vinyl conformation upon heme iron reduction in the presence of substrate seems to correlate well with the heme redox potential and the size of residue 393. In the absence of substrate, heme reduction induces a similar conformational change, but the crowded vibrational region complicates a deconvolution analysis. Furthermore, the substrate-bound form of the enzyme is the physiologically relevant one that undergoes heme reduction.

DISCUSSION

Our resonance Raman results on the ferric and ferrous forms of the WT P450 BM3 heme domain in the presence and absence of substrate are very similar to those reported before (*46*, *47*, *55*, *56*, *58*). Our goal was to investigate the effect of mutation of F393 on the structure of the heme cofactor and its interactions with the protein environment and to test whether observed changes correlate with the modification of the heme iron reduction potential in the mutants. Our data show that the mutations do not have a significant effect on the heme core size marker bands. Although reduction of the heme results in the enhancement of out-of-plane vibrational modes, their intensities are relatively the same for the different mutants, suggesting that the mutations do not significantly affect the heme planarity. Furthermore, changes in the ν_3, ν_{10}, and ν_8 vibrations that are markers of heme ruffling suggest that only minor changes in heme ruffling may occur, and we conclude that these changes play at best a minor role in modifying the heme redox potential in the F393 mutants of P450 BM3 (*20*−*22*, *70*, *75*, *76*). Mutation of F393 does induce changes in thiolate σ-electron donation and in vinyl group conformations following heme reduction, and in the extent of propionate hydrogen bonding following substrate binding. It was surprising to find that the Fe−S stretching frequency was not affected by the mutations despite the large change in redox potential. These observations will be discussed in more detail.

Bonding Interaction to the Redox Center. The proximal cysteine thiolate ligand plays a critical role in the reaction cycle of P450 enzymes and is thought to provide a "push effect" by strongly donating electron density to the heme iron (*4*, *77*−*80*). This results in a much more negative redox potential in P450 enzymes with respect to hemeproteins with a proximal histidine (*2*, *4*, *23*−*25*); e.g., in Mb, replacement of the proximal histidine with cysteine decreases its redox potential by 280 mV (*23*). The electron density between the heme iron and the thiolate ligand can be assessed by the strength of the Fe−S bond or the ν(Fe−S) frequency. In the WT P450 BM3 heme domain, ν(Fe−S) is at 356 cm^{-1}. Despite the large effect of the F393 mutations on the heme redox potential (*7*), ν(Fe−S) is not significantly affected by the mutations. This indicates that the strength of and the electron density in the Fe−S bond remain unchanged upon mutation of F393 and argues against the use of the Fe−S stretching frequency of the ferric 5C/HS enzyme as a reliable indicator of the heme redox potential in P450 BM3 and in other hemothiolate proteins as indicated by recent work on P450cam proximal site mutants (*27*, *28*).

In the reduced, substrate-free heme domains and to a lesser extent in their substrate-bound forms, the σ-electron donation of the thiolate to the heme iron is sensitive to the F393 mutations, as evidenced by the change in the ν_4 frequency. This frequency increases from F393W to WT to F393H to F393A, suggesting a decrease in $Fe^{II}d_\pi$ back bonding to the porphyrin ring due to a decrease in thiolate σ-electron donation to the ferrous iron (*61*), and is supported by the concomitant decrease in the ν_8 frequency. The decrease in σ-electron donation correlates with an increase in the heme redox potential. The F393Y mutant has the lowest ν_4 frequency and does not fit this correlation for reasons that are currently not clear. The decrease in σ-electron donation by the thiolate ligand may indicate that hydrogen bonding to the thiolate has increased, but the absence of a change in ν(Fe−S) in the F393 mutants argues against significant changes in hydrogen bonding. This is not too surprising because mutations affecting the proximal hydrogen-bonding network of P450cam and experiments on model compounds showed only minor effects of hydrogen bonding on both the ν(Fe−S) frequency and the heme redox potential compared to the potentials observed in the F393 mutants (*7*, *27*−*29*). Large changes in the heme redox potential due to hydrogen bond formation, i.e., lowering of σ-electron donation, are expected to induce a significant change in the ν(Fe−S) frequency, as we proposed for eNOS (*26*). In P450 BM3, mutation of F393 results in significant modification of the heme redox potential without a change in Fe−S bond strength in its ferric 5C/HS form. Since ν(Fe−S) can only be determined for 5C/HS ferric heme and the F393 mutations affect σ-electron donation in the reduced form of the heme domains, we cannot rule out that the Fe−S bond strength is modified in the 5C/HS reduced state of the heme, thereby affecting σ-electron donation.

Effect of F393 Mutation on Propionate Conformation. Our results indicate that heme iron reduction has a minor effect on the conformation of the propionate groups. However, addition of substrate induces a conformational change in one

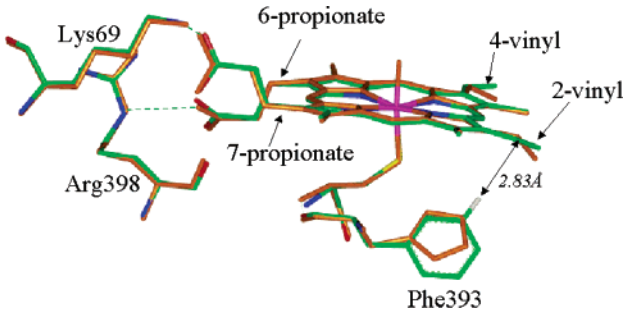

FIGURE 7: Superposition of the heme cofactors of resting WT (green) and F393H (orange) P450 BM3 (refs *5* and *7*, PDB entries 2HPD and 1JME). Protein environment (Lys69, Phe/His393, Arg398, and Cys400) near the heme cofactors are shown together. Dotted lines indicate the hydrogen bonding between the heme propionate groups and the protein environment. A hydrogen atom is shown at the Cϵ1 position of the Phe393 in WT enzyme to reflect steric interaction within the 2-vinyl group. Protonation of the His393 occurs at the Nδ1 position, so there is no hydrogen atom attached to the Nϵ2 in F393H.

of the propionate groups. In the absence of substrate, only one propionate bending vibration is observed at 380 cm-^{1} in both redox states of the P450 BM3 heme domain and its F393 mutants, indicative of strong hydrogen bonding interactions with the protein matrix (*64*−*66*). This conclusion is supported by the crystal structures of the WT enzyme and the F393H mutant, which show strong protein hydrogen bonds to both propionate groups (*5*, *7*, Figure 7). Substrate binding induces a conformational change in one propionate group as indicated by a new bending vibration at 366 cm^{-1} (373 cm^{-1} in reduced form), which has lost or reduced hydrogen bonding interaction with the protein matrix (*63*−*66*). X-ray structural data (*81*, PDB entry 1FAG) show that substrate-binding breaks the hydrogen bond between the 7-propionate and Lys69, and we associate it with the 366 cm^{-1} bending mode. The extent of loss of hydrogen bonding upon substrate binding is sensitive to the size of residue 393 and increases as follows: F393A $\sim$ F393H < F393Y $\sim$ WT < F393W. The heme redox potential changes in the same order, which suggests a correlation with propionate conformation.

The effect of propionate conformation on the heme redox potential has been proposed before, and Mauk and coworkers showed that esteration and delectation of one or both propionates increases the heme redox potential by about 60 and 25 mV, respectively, and proposed that the negative charge of the propionates can stabilize the heme iron in its ferric state and lower its redox potential (*35*−*38*). Anionation of the propionate groups can decrease the heme redox potential by up to 100 mV (*40*). However, Walker and coworkers showed that elongation but not shortening of the propionate group by one carbon results in a 10 mV decrease in redox potential and concluded that the propionate groups play only a minor role in modifying the heme redox potential (*39*). A recent computational study supports the idea that propionates can lower the redox potential in heme proteins (*82*).

The LMCT band is sensitive to changes in charge in the distal pocket and shifts from 632 to 622 nm in the Mb V68D distal pocket mutant with a 200 mV decrease in heme redox potential (*16*). In the P450 BM3 heme domains, the LMCT band shows only a small red shift, which is larger in F393A and F393H than in F393W and F393Y, in agreement with an increasing redox potential. Unfortunately, we could not determine the position of the MLCT band in WT accurately, which makes it difficult to relate its shift to the introduction of negative charge in the distal pocket related to a change in propionate conformation or heme redox potential.

Our results do show a correlation between the conformation of the propionate groups and the heme redox potential, but it is difficult to quantify the contribution to the redox potential. Since the conformation is only affected upon substrate binding and the F393 mutations affect the heme redox potential also in the absence of substrate, we conclude that the contribution of the propionate groups to the change in redox potential is relatively small, in agreement with Walker and co-workers and with the small shift in the LMCT band (*39*). We do expect some contribution of the propionate groups to stabilization of the ferric heme in F393W and to destabilization in F393H and F393A relative to WT enzyme, in agreement with the observed redox potentials (*7*).

Effect of F393 Mutation on Vinyl Conformation. On the basis of the stretching and bending vibrations of the vinyl groups, we have identified in-plane and an out-of-plane vinyl conformers, as has been reported before only on the basis of the stretching modes (*47*, *56*). Our analysis will focus on the behavior of the vinyl bending modes. In contrast to the propionate groups, the conformation of the vinyl groups is less sensitive to substrate binding but very sensitive to heme iron reduction. In the resting heme domain, mutation of F393 results in a change in vinyl bending frequencies and intensities. We observe no changes in heme skeletal vibrations following mutation of F393 and rule out that the frequency changes are induced by changes in electron density or heme planarity. We attribute them to a change in the direct protein environment of the vinyl groups. This is supported by the observation that the frequency increases with decreasing size of residue 393 as follows: F393W < WT $\sim$ F393Y < F393H < F393A. The fact that F393 is in van der Waals contact with the 2-vinyl group (Figure 7) underscores this conclusion. In F393A and F393H, the vinyl bending frequencies are higher, suggesting that the vinyl groups in these mutants are rotated more out of the heme plane relative to the WT enzyme. This is supported by the observation of an out-of-plane vinyl stretching mode at 1632 cm^{-1} in these two mutants, which has less intensity in the WT enzyme and the two other mutants. X-ray data show that the torsion angles of the 2- and 4-vinyl groups change from −12° and −6° above the heme plane toward the distal side in WT to 28° and 26° below the heme plane toward the proximal side in F393H (*5*, *7*), supporting our analysis of the RR data. However, the X-ray data only show one dominant structure, while the RR experiments probe the ensemble of possible structures in solution, which may result in minor discrepancies.

Heme iron reduction significantly enhances the bending mode of the in-plane vinyl conformer both in the absence and presence of substrate, suggesting that the in-plane conformation is energetically more favorable. This change in vinyl conformation has been observed before on the basis of the vinyl stretching vibration in P450 BM3, and it was suggested that it might be involved in regulation of enzyme reactivity (*47*, *56*). Recent structural data of P450cam also show a significant change in the vinyl conformations,

especially the 4-vinyl assumes an in-plane conformation following one-electron reduction (*83*, PDB entries 1DZ4 and 1DZ6), though these data do not necessarily reflect the conformations populated in solution. Deconvolution of the vinyl bending modes of the substrate-bound heme domains shows that the population of the in-plane vinyl conformer is larger in heme domains in which F393 is replaced with a less bulky side chain (Table 2). We propose that our data indicate that reduced heme energetically favors the in-plane vinyl conformation but that steric hindrance of the residue at position 393 may affect such a conformational change. Flexibility of the vinyl groups in P450 BM3 has been pointed out before (*47*, *56*, *84*). It has been suggested that the vinyl groups are forced into the heme plane by a change in heme−substrate distance upon heme reduction (*85*). However, in the substrate-free heme domains, we observe the same conformational change of the vinyl groups following heme reduction, which indicates that substrate binding plays only a minor role in this process.

Walker and co-workers have convincingly argued that an in-plane vinyl conformer can withdraw more electron density from the heme iron than an out-of-plane conformer by conjugating with the porphyrin ring, raising the heme redox potential (*39*, *43*). Calculations performed on styrene and 4-vinylpyridine have confirmed the electron withdrawing capability of vinyl groups in their planar conformation (*86*, *87*). Our data support Walker's proposal and indicate that the conformation of the vinyl groups can modify the electron density on the heme iron and its redox potential. The trend that we observe is that heme domains with a higher redox potential have a larger in-plane vinyl population. In that case, the vinyl groups withdraw more electron density from the heme iron through $Fe^{II}d_{\pi}$-electron back bonding to the porphyrin ring. Our observation of a higher ν_4 frequency and a lower ν_8 frequency in the substrate-free and -bound ferrous heme domains with higher redox potentials is in agreement with reduced electron density on the heme iron due to increased conjugation of the vinyl groups with the porphyrin ring and does not require hydrogen bonding to the thiolate ligand to explain the reduced electron density on the heme iron, though that cannot be ruled out completely.

We propose that modulation of the heme redox potential by residue 393 in P450 BM3 heme domains is in part due to the ability of the vinyl groups to move into the heme-plane upon reduction of the heme iron. This ability is affected by the size of the residue at position 393 and is better for Ala and worse for Trp, resulting in the higher and lower redox potential, respectively, with respect to WT. The observation that the F393 mutations affect the heme cofactor in mainly its reduced state is in agreement with previous work by Ost et al. (*7*). Our data provide evidence for the original proposal that the heme redox potential is affected by the conformation of the vinyl groups (*39*, *41*, *43*) and the proposal by Hudeček et al. that these conformational changes may regulate reactivity in P450 BM3 (*47*). However, the contribution of one vinyl group to the heme redox potential has an upper limit of about 50 mV (*39*, *43*), which cannot explain the large difference in redox potential between F393W and F393A. Therefore, other factors such as hydrogen bonding to the proximal thiolate may still play a role in regulating the heme redox potential. Although we do not observe evidence for modification of the Fe−S bond in the ferric 5C/HS enzymes, we cannot rule out that such a modification occurs in the reduced state of the enzyme. Further experiments and a computational study are underway to test our model.

CONCLUSIONS

Our resonance Raman investigation of the heme cofactor in the WT heme domain of P450 BM3 and its F393 mutants has revealed that several heme structural changes correlate to the size of residue 393 and to the change in heme redox potential. Surprisingly, the ν(Fe−S) frequency does not change, indicating that the Fe−S bond in substrate-bound, ferric P450 BM3 is not affected significantly by the mutation and is not a reliable indicator of the heme iron redox potential in the P450 BM3 heme domain. With increasing redox potential, we have observed a decrease in the loss of propionate hydrogen bonding in the presence of substrate and an increase in the population of the in-plane vinyl conformer upon reduction of the heme iron. Although the conformational change of one propionate group, presumably the 7-propionate, correlates well with the heme redox potential, the propionates seem to have only a minor effect on the heme redox potential. The population of in-plane vinyl conformer in the reduced heme domains shows a strong correlation with the heme redox potential. We conclude that the in-plane vinyl groups withdraw more electron density from the heme iron through $Fe^{II}d_{\pi}$ back bonding to the porphyring ring than the out-of-plane conformer, which is supported by the observed decrease in Fe^{II} electron density, as judged from the ν_4 frequency. The fact that smaller residues at position 393 have a larger vinyl in-plane population and a higher heme redox potential suggests that residue 393 may play an important role in controlling the electronic properties of the heme through steric interactions between the heme cofactor and the protein matrix. Although the correlation between the vinyl group conformations and the change in heme redox potential is striking, the vinyl groups alone cannot explain the entire range of redox potentials in the F393 mutants of the P450 BM3 heme domain, and other contributing factors are not ruled out.

SUPPORTING INFORMATION AVAILABLE

The absorption spectra, high-frequency resonance Raman spectra, and deconvolution spectra of the vinyl bending modes are available free of charge via the Internet at http://pubs.acs.org.

REFERENCES

1. Munro, A. W., and Lindsay, J. G. (1996) *Mol. Microbiol. 20*, 1115−1125.
2. Ortiz de Montellano, P. R., Ed. (1986) in *Cytochrome P-450: Structure, Mechanism and Biochemistry*, Plenum Press, New York.
3. Munro, A. W., Leys, D. G., McLean, K. J., Marshall, K. R., Ost, T. W. B., Daff, S., Miles, C. S., Chapman, S. K., Lysek, D. A., Moser, C. C., Page, C. C., and Dutton, P. L. (2002) *Trends Biochem. Sci. 27*, 250−257.
4. Sono, M., Roach, M. P., Coulter, E. D., and Dawson, J. H. (1996) *Chem. Rev. 96*, 2841−2887.
5. Ravichandran, K. G., Boddupalli, S. S., Hasemann, C. A., Peterson, J. A., and Deisenhofer, J. (1993) *Science 261*, 731−736.
6. Nelson, D. R., Koymans, L., Kamataki, T., Stegeman, J. J., Feyereisen, R., Waxman, D. J., Waterman, M. R., Gotoh, O., Coon, M. J., Estabrook, R. W., Gunsalus, I. C., and Nebert, D. W. (1996) *Pharmacogenetics 6*, 1−42.

7. Ost, T.W. B., Miles, C. S., Munro, A. W., Murdoch, J., Reid, G. A., and Chapman, S. K. (2001) *Biochemistry 40*, 13421−13429.
8. Ost, T.W. B., Munro, A. W., Mowat, C. G., Taylor, P. R., Pesseguiero, A., Fulco, A. J., Cho, A. K., Cheesman, M. A., Walkinshaw, M. D., and Chapman, S. K. (2001) *Biochemistry 40*, 13430−13438.
9. Moore, G. R., Pettigrew, G. W., and Rogers, N. K. (1986) *Proc. Natl. Acad. Sci. U.S.A. 83*, 4998−4999.
10. Lewis, D. F. V., Ed. (1996) in *Cytochromes P450: Structure, Function and Mechanism*, Taylor & Francis, Bristol, PA.
11. Kassner, R. (1972) *Proc. Natl. Acad. Sci. U.S.A. 69*, 2263−2267.
12. Churg, A. K., and Warshel, A. (1986) *Biochemistry 25*, 1675−1681.
13. Caffrey, M. S., Daldal, F., Holden, H. M., and Cusanovich, M. A. (1991) *Biochemistry* 30, 4119−4125.
14. Paoli, M., Marles-Wright, J., and Smith, A. (2002) *DNA Cell Biol.* 21, 271−280.
15. Varadarajan, R., Zewert, T. E., Gray, H. B., and Boxer, S. G. (1989) *Science 243*, 69−72.
16. Varadarajan, R., Lambright D. G., and Boxer, S. G. (1989) *Biochemistry 28*, 3771−3781.
17. Jones, D. K., Patel, N., and Lloyd Raven, E. (2002) *Arch. Biochem. Biophys. 400*, 111−117.
18. Atamian, M., and Bocian, D. F. (1987) *Biochemistry 26*, 8319−8326.
19. Walker, F. A., Emrick, D., Rivera, J. E., Hanquet, B. J., and Buttlaire, D. H. (1988) *J. Am. Chem. Soc. 110*, 6234−6240.
20. Jentzen, W., Simpson, M. C., Hobbs, J. D., Song X., Ema, T., Nelson, N. Y., Medforth, C. J., Smith, K. M., Veyrat, M., Mazzanti, M., Ramasseul R., Marchon, J. C., Takeuchi, T., Goddard, W. A., III, and Shelnutt, J. A. (1995) *J. Am. Chem. Soc 117*, 11085−11097.
21. Ma, J. G., Zhang, J., Franco, R., Jia, S. L., Moura, I., Moura, J. J. G., Kroneck, P. M. H., and Shelnutt, J. A. (1998) *Biochemistry 37*, 12431−12442.
22. Ma, J.-G., Vanderkooi, J. M., Zhang, J., Jia, S.-L., and Shelnutt, J. A. (1999) *Biochemistry 38*, 2787−2795.
23. Adachi, S., Nagano, S., Ishimori, K., Watanabe, Y., Morishima, I., Egawa, T., Kitagawa, T., and Makino, R. (1993) *Biochemistry 32*, 241−252.
24. Liu, Y., Moenne-Loccoz, P., Hildebrand, D. P., Wilks, A., Loehr, T. M., Mauk, A. G., and Ortiz de Montellano, P. R. (1999) *Biochemistry 38*, 3733−3743.
25. Auclair, K., Moenne-Loccoz, P., and Ortiz de Montellano, P. R. (2001) *J. Am. Chem. Soc. 123*, 4877−4885.
26. Schelvis, J. P. M., Berka, V., Babcock, G. T., and Tsai, A. L. (2002) *Biochemistry 41*, 5695−5701.
27. Tosha, T., Yoshioka, S., Hori, H., Takahashi, S., Ishimori, K., and Morishima, I. (2002) *Biochemistry 41*, 13883−13893.
28. Yoshioka, S., Tosha, T., Takahashi, S., Ishimori, K., Hori, H., and Morishima, I. (2002) *J. Am. Chem. Soc. 124*, 14571−14579.
29. Suzuki, N., Higuchi, T., Urano Y., Kikuchi K., Uekusa H., Ohashi Y., Uchida T., Kitagawa T., and Nagano, T (1999) *J. Am. Chem. Soc 121*, 11571−11572.
30. Champion, P. M., Stallard, B. R., Wagner, G. C., and Gunsalus, I. C. (1982) *J. Am. Chem. Soc. 104*, 5469−5472.
31. Bangcharoenpaurpong, O., Champion, P. M., Hall, K. S., and Hager, L. P. (1986) *Biochemistry 25*, 2374−2378.
32. Bangcharoenpaurpong, O., Champion, P. M., Martinis, S. A., and Sligar, S. G. (1987) *J. Chem. Phys. 87*, 4273−4284.
33. Unno, M., Christian, J. F., Benson, D. E., Gerber, N. C., Sligar, S. G., and Champion, P. M. (1997) *J. Am. Chem. Soc. 119*, 6614−6620.
34. Chen, Z. C., Wang, L. H., and Schelvis, J. P. M (2003) *Biochemistry 42*, 2542−2551.
35. Argos, P., and Mathews, S. (1975) *J. Biol. Chem. 250*, 747−751.
36. Reid, L. S., Taniguchi, V. T., Gray, H. B., and Mauk, A. G. (1982) *J. Am. Chem. Soc. 104*, 7516−7519.
37. Reid, L. S., Mauk, M. R., and Mauk, A. G. (1984) *J. Am. Chem. Soc. 106*, 2182−2185.
38. Funk. W. D., Lo, T. P., Mauk, M. R., Brayer, G. D., MacGillivray, R. T. A., and Mauk, A. G. (1990) *Biochemistry 29*, 5500−5508.
39. Lee, K. B., Jun, E., La Mar, G. N., Rezzano, I. N., Pandey, R. K., Smith, K. M., Walker, F. A., and Buttlaire, D. H. (1991) *J. Am. Chem. Soc. 113*, 3576−3583.
40. Das, D. K., and Medhi, O. K. (1998) *J. Inorg. Biochem. 70*, 83−90.
41. Satterlee, J. D., and Erman, J. E. (1983) *J. Biol. Chem. 258*, 1050−1056.
42. Balke, V. L., Walker, F. A., and West. J. T. (1985) *J. Am Chem. Soc. 107*, 1226−1233.
43. Reid, L. S., Lim, A. R., and Mauk, A. G. (1986) *J. Am. Chem. Soc 108*, 8197−8201.
44. La Mar, G. N., Budd, D. L., Smith, K. M., and Langry, K. C. (1980) *J. Am. Chem. Soc. 102*, 1822−1827.
45. Macdonald, I. D. G., Smith, E. W., and Munro, A. W. (1996) *FEBS Lett. 396*, 196−200.
46. MacDonald, I. D. G., Munro, A. W., and Smith, W. E. (1998) *Biophys. J.*, 3241−3249.
47. Hudeček, J., Anzenbacherova, E., Anzenbacher, P., Munro, A. W., and Hildebrandt, P. (2000) *Arch. Biochem. Biophys. 383*, 70−78.
48. Anzenbacher, P., and Huděcek, J. (2001) *J. Inorg. Biochem. 87*, 209−213.
49. Spiro, T. G., Ed. (1988) in *Biological Applications of Raman Spectroscopy, Vol. 3: Resonance Raman Spectra of Heme and Metalloproteins*, Wiley & Sons, New York.
50. Choi, S., and Spiro, T. G. (1983) *J. Am. Chem. Soc. 105*, 3683−3692.
51. Choi, S., Lee, J. J., Wei, Y. H., and Spiro, T. G. (1983) *J. Am. Chem. Soc. 105*, 3692−3707.
52. Hu, S., Smith, K. M., and Spiro, T. G. (1996) *J. Am. Chem. Soc. 118*, 12638−12646.
53. Hu, S., Morris, I. K., Singh, J. P., Smith, K. M., and Spiro, T. G. (1993) *J. Am. Chem. Soc. 115*, 12446−12458.
54. Noble, M. A., Miles, C. S., Chapman, S. K., Lysek, D. A., Mackay, A. C., Reid, G. A., Hanzlik, R. P., and Munro, A. W. (1999) *Biochem. J. 339*, 371−379.
55. Deng, T. J., Proniewicz, L. M., Kincaid, J. R., Yeom, H., Macdonald, I. D. G., and Sligar, S.G. (1999) *Biochemistry 38*, 13699−13706.
56. Hudeček, J., Baumruk, V., Anzenbacher, P., and Munro, A. W. (1998) *Biochem. Biophys. Res. Commun. 243*, 811−815.
57. Kalsbeck, W. A., Ghosh, A., Pandey, R. K., Smith, K. M., and Bocian, D. F., (1995) *J. Am. Chem. Soc. 117*, 10959−10968.
58. Sligar, S.G. (1976) *Biochemistry 15*, 5399−5406.
59. Wells, A. V., Li, P., Champion, P. M., Martinis, S. A., and Sligar, S. G. (1992) *Biochemistry 31*, 4384−4393.
60. Hildebrandt, P., Greinert, R., Stier, A., and Taniguchi, H. (1989) *Eur. J. Biochem. 186*, 291−302.
61. Anzenbacher, P., Evangelista-Kirkup, R., Schenkman, J., and Spiro, T. G. (1989) *Inorg. Chem. 28*, 4491−4495.
62. Miles, J. S., Munro, A. W., Rospendowski, B. N., Smith, W. E., McKnight, J., and Thomson, A. J. (1992) *Biochem. J. 288*, 503−509.
63. Cerda-Colon, J. F., Silfa, E., and Lopez-Garriga, J. (1998) *J. Am. Chem. Soc. 120*, 9312−9317.
64. Peterson, E. S., Friedman, J. M., Chien, E. Y. T., and Sligar S. G. (1998) *Biochemistry 37*, 12301−12319.
65. Nagai, M., Aki, M., Li, R., Jin, Y., Sakai, H., Nagatomo, S., and Kitagawa, T. (2000) *Biochemistry 39*, 13093−13105.
66. Hildebrand, D. P., Burk, D. L., Maurus, R., Ferrer, J. C., Brayer, G. D., and Mauk, A. G. (1995) *Biochemistry 34*, 1997−2005.
67. Evans, S. V., and Brayer, G. D. (1990) *J. Mol. Biol. 213*, 885−897.
68. Maurus, R., Overall, C. M., Bogumil, R., Luo, Y., Mauk, A. G., Smith, M., and Brayer, G. D. (1997) *Biochim. Biophys. Acta 1341*, 1−13.
69. Smulevich, G., Hu, S. Z., Rodgers, K. R., Goodin, D. B., Smith, K. M., and Spiro, T. G. (1996) *Biospectroscopy 2*, 365−376.
70. Czernuszewicz, R. S., Li, X. Y., and Spiro, T. G. (1989) *J. Am. Chem. Soc. 111*, 7024−7031.
71. Matsunaga, I., Yamada, A., Lee, D. S., Obayashi, E., Fujiwara, N., Kobayashi, K., Ogura, H., and Shiro, Y. (2002) *Biochemistry 41*, 1886−1892.
72. Lee, D. S., Yamada, A., Sugimoto, H., Matsunaga, I., Ogura, H., Ichihara, K., Adachi, S. I., Park, S. Y., and Shiro, Y (2003) *J. Biol. Chem. 278*, 9761−9767.
73. Munro, A. W., Lindsay, J. G., Coggins, J. R., MacDonald, I., Smith, W. E., and Rospendowski, B. N. (1993) *Biochem. Soc. Trans. 22*, 54S.
74. Green, E. L., Taoka, S., Banerjee, R., and Loehr, T. M. (2001) *Biochemistry 40*, 459−463.
75. Shelnutt, J. A., Medforth, C. J., Berber, M. D., Barkigia K. M., and Smith, K. M. (1991) *J. Am. Chem. Soc 113*, 4077−4087.
76. Alden, R. G., Crawford, B. A., Doolen, R., Ondrias, M. R., and Shelnutt, J. A. (1989) *J. Am. Chem. Soc. 111*, 2070−2072.
77. Green, M. T. (1998) *J. Am. Chem. Soc. 120*, 10772−10773.

78. Green, M. T. (1999) *J. Am. Chem. Soc. 121*, 7939−7940.
79. Daiber, A., Nauser, T., Takaya, N., Kudo, T., Weber, P., Hultschig, C., Shoun, H., and Ullrich, V. (2002) *J. Inorg. Biochem. 88*, 343−352.
80. De Visser, S. P., Ogliaro, F., Sharma, P. K., and Shaik, S. (2002) *J. Am. Chem. Soc. 124*, 11809−11826.
81. Li, H., and Poulos, T. L. (1997) *Nat. Struct. Biol. 4*, 140−146.
82. Mao, J, Hauser, K., and Gunner, M. R. (2003) *Biochemistry 42*, 9829−9840.
83. Schlichting, I, Berendzen, J., Chu, K., Stock, A. M., Maves, S. A., Benson, D. E., Sweet, R. M., Ringe, D., Petsko, G. A., and Sligar, S. G. (2000) *Science 287*, 1615−1622.
84. Anzenbacherova, E., Nicole, Bec, Anzenbacher, P., Hudeček, J., Souček, P, Jung, C., Munro, A. W., and Lange, R. (2000) *Eur. J. Biochem. 267*, 2916−2920.
85. Modi, S., Sutcliffe, M. J., Primrose, W. U., Lian, L. Y., and Robert, G. C. K. (1996) *Nat. Struct. Biol. 3*, 414−417.
86. Bock, C. W., Trachtman, M., and George, P. (1985) *Chem. Phys. 93*, 431−443.
87. Bock, C. W., Trachtman, M., and George, P. (1986) *Chem. Phys. 105*, 107−116.

BI034920G